Construction and Building Materials 289 (2021) 123154

Contents lists available at ScienceDirect

Construction and Building Materials

journal homepage: www.elsevier.com/locate/conbuildmat

Effect of macro polypropylene, polyamide and steel fibers on the residual properties of SCC at ambient and elevated temperatures

Soner Guler [a,*], Zehra Funda Akbulut [a], Hocine Siad [b], Mohamed Lachemi [b]

[a] Faculty of Engineering, University of Van Yuzuncu Yıl, Turkey
[b] Faculty of Engineering and Architectural Science, Ryerson University, Toronto, Canada

HIGHLIGHTS

- Macro PP, PA and ST fibers were investigated in SCCs exposed to temperatures up to 800 °C.
- The use of macro-ST resulted in higher workability reductions than PP and PA.
- Macro PA caused greater residual toughness results than PP.
- Macro ST fibers are more effective in improving the mass loss, RCS, RFS and RT of SCCs.
- 0.3% PP and PA fibers were proven to generate higher post-peak RT capacity at 300 °C.

ARTICLE INFO

Article history:
Received 21 November 2020
Received in revised form 17 March 2021
Accepted 19 March 2021

Keywords:
Self-compacting concrete
Steel fiber
Synthetic fiber
Residual strength
Residual toughness
Elevated temperature

ABSTRACT

This paper considers the effect of equivalent macro size fibers of polypropylene (PP), polyamide (PA) and steel (ST) on the properties of reinforced self-compacting concrete (FRSCC) exposed to normal and elevated temperatures. Different fiber concentrations of 0%, 0.3%, 0.6% and 1% were investigated under temperatures of 20 °C, 300 °C, 500 °C and 800 °C. Mass loss, residual compressive strength (RCS), residual flexural strength (RFS), toughness indices (TI), residual strength factors (RSF) and residual toughness (RT) capacities of FRSCCs were studied at hardened state based on their initial results at ambient curing. Meanwhile, slump-flow diameter, T_{500} time and L-box parameters were also tested at fresh state. In addition, the microstructural changes due to the use of various fibers and temperatures were examined by scanning electron microscope (SEM) analysis. The effect of macro PA and PP was comparable in terms of their minor influence on the mass loss, RCS and RFS of FRSCC compositions. However, macro PA presented greater contribution than PP in preserving the toughness capacity, particularly in the post-peak stage. Unlike PA and PP, the use of macro ST fibers caused noticeable increments in RFS and RT capacities. The superior outcome of using macro ST was confirmed through its higher effect in mitigating the crack formation of FRSCC, especially under elevated temperatures of 500 °C and 800 °C.

© 2021 Elsevier Ltd. All rights reserved.

1. Introduction

Self-compacting concrete (SCC) is known as a relatively recent generation of fluid cementitious materials [1,2] which have a considerable ability to settle with its own weight [3,4]. It was also presented with many advantages over normal concretes (NC), such as shortening the manufacturing time, reducing the labor cost, and reducing noise pollution in construction activities [5–7]. However, as NC, standard SCCs has also semi-brittle behaviors, which affected negatively their frequent use in different structural elements and geometric sections. Thus, the notion of fiber reinforced SCC (FRSCC) was emerged as a solution to slow down the rapid and uncontrolled progression of cracks in SCC compositions [8–13]. Steel fibers (SF) were the most used in FRSCCs due to their high tensile and elasticity modulus. Nevertheless, their low corrosion resistance and increased volumetric ratio have encouraged researchers to seek alternatives by using synthetic fibers such as polyolefin, polypropylene (PP), polyethylene (PE), and aramid [8,15–18]. Indeed, synthetic fibers, usually obtained from synthesized polymers using chemical extraction methods, are presented with high corrosion resistance, light weight, and lower cost compared to steel fibers [19–24]. Also, when used in SCC, they provided equivalent fresh and mechanical performances than SF [18,24]. As well as the room condition testing, the effect of incorporating SF and polymer-based synthetic fibers on the residual capacities of

* Corresponding author.
E-mail address: gulersoner@yyu.edu.tr (S. Guler).

https://doi.org/10.1016/j.conbuildmat.2021.123154
0950-0618/© 2021 Elsevier Ltd. All rights reserved.

SCC was also considered under high temperature exposure [25–33]. Sideris et al. [25] tested the effect of adding PP fibers of 6 mm and 12 mm length and a dosage of 1 kg/m^3 on the mechanical and spalling resistance of limestone filler-SCC subjected to temperatures of 300 °C and 600 °C. Both PP fibers were presented to be effective in preventing the spalling of specimens at various temperatures; nevertheless, they did not provide an important contribution in the residual compressive and tensile strength of SCC. Eidan et al. [26] also investigated the effect of fiber length and dosage on the residual mechanical properties of PP-based SCCs prepared without mineral addition and exposed to 400 and 600 ℃ temperatures. They used 6 mm and 12 mm lengths and concentrations of 1, 1.5 and 2 kg/m^3 of PP fibers and concluded that the higher fiber length at maximum concentration resulted in better recovery of the initial compressive and splitting tensile strengths after exposure to 600 ℃ heating–cooling cycle. Sadrmomtazi et al., [27] studied the effect of adding steel fibers and up to 30% of fly ash on the properties of limestone powder-based SCCs exposed to temperatures of 23–600 °C. They showed that using ST fibers with a length of 25 mm contributed in maintaining 24% of the compressive strength; however, adding 30% fly ash was more effective by up to 47%. They also concluded that ST fibers are useful in preventing crack spreading and maintaining the residual strength, especially under 400 °C. Ding et al. [28] analyzed the effect of PP and ST fibers in single and hybrid form on the residual capacities, failure pattern and fracture energy of fly ash-SCC after exposure to 300, 600 and 900 ℃. They used different PP and ST lengths of 15 mm and 35 mm respectively, and showed that the single use of PP and hybrid PP-ST fibers resulted in maintaining higher fracture energy than SF under higher temperatures. Mahapatra and Barai [29] and Xargay et al. [30] investigated the effect of hybrid macro ST and micro PP fibers and elevated temperatures of maximum 600 °C on the average residual properties of SCC incorporated fly ash and blast furnace slag. Their results revealed that the use of hybrid form ST-PP fibers highly reduced the negative effect of elevated temperatures on the compressive strengths and external- and post-cracking of SCC mixes. PP fibers, which are more used compared to other synthetic fibers, were reported to reduce the risk of spalling of SCC exposed to elevated temperatures. Although, these studies didn't show a strict agreement about the negative or positive effect of PP fibers due to their melting temperature and related supplementary porosity, they generally presented them with insignificant role on the residual performance of SCCs [31–33]. Also, they confirmed the importance of the type, dosage and properties of fibers on the residual properties of SCCs under elevated temperatures. Naturally and artificially made amide bonds-based Polyamide fibers (PA), presented with higher durability, strength and elastic modulus than other synthetic fibers [34,35], were also incorporated in cementitious composites [36–38]. They were shown to improve the mixing process of fiber reinforced concretes (FRC) and to increase their fiber/matrix bond and post-cracking behavior compared to SF [39,40] and to display better mechanical strengths and freeze–thaw resistance than PP [41–43]. However, no studies in the literature were found about the use of PA-type fibers in SCC compositions, though its cheap cost and higher mechanical properties and melting temperature than PP.

1.1. Research significance

The investigation of the fresh and hardened concrete properties of different types of fibers reinforced SCC has been the focus of interest of many researchers so far. Thus, the effects of single and hybrid use of macro sized ST fibers (up to 35 mm) and micro sized synthetic fibers (6 and 12 mm) on the workability and strength properties of SCC have been mostly investigated. However, the effects of steel and synthetic fibers with longer and greater aspect ratio and equivalent macro size on the workability, residual strength and residual toughness capacity of SCC exposed to high temperatures are not considered in the literature. In addition, the use of PA-type synthetic fibers in SCC compositions is very limited, though the possible advantages of this fiber regarding its cheap cost and higher mechanical properties and melting temperature compared to PP. In this study, it was first tried to determine how the macro-sized ST, PP and PA fibers with lengths of 60, 54, and 40 mm respectively, affect the workability, strength and toughness capacity of SCC under room conditions. Secondly, it has been tried to determine to what extent the macro ST, PP and PA fibers contribute to the mass loss, residual strength and residual toughness capacities of SCC exposed to elevated temperatures. Also, SEM images were taken from ST, PA and PP reinforced SCC samples at room conditions and elevated temperatures to examine the changes caused by the high temperature conditions.

2. Experimental program

2.1. Materials

In the preparation of SCC mixtures, CEM I 42.5 R type cement and F class fly ash were used as binders in accordance with EN 197-1 [44] standard. Two different size crushed aggregates of 0–5 mm and 5–12 mm were used as sand and gravel in all SCC mixtures. Steel fibers (ST) were hooked-end with a length of 60 mm, whereas polypropylene (PP) and polyamide (PA) were monomer propylene- and repeating units' macromolecule- type synthetic fibers with lengths of 40 and 54 mm respectively. These lengths were selected to be as close as possible based on their commercial availability. Their physical and mechanical properties are given in Table 1, with melting temperatures of 1539 °C, 160 °C and 256 °C for SF, PP and PA respectively. The visual appearance of fibers is shown in Fig. 1. In addition, MasterGlenium ACE 450 polycarboxylic ether-based superplasticizer (SP) was used to improve the workability of SCCs.

2.2. Mix design and preparation of mixes

SCC mixes were prepared in accordance to EFNARC standard [45]. A total of 10 concrete mixes were prepared, one of which was control and 9 were FRSCC mixes, as shown in Table 2. The total amount of binder (cement + fly ash) was determined as 500 kg/m^3 and the water/cement (w/c) ratio was 0.48 in all SCC mixtures. The fibers were incorporated at 0.3%, 0.6% and 1% by volume in FRSCC_0.3, FRSCC_0.6 and FRSCC_1 respectively, while the control concrete was produced without fibers. SP was used at the rate of 1% by weight of cement in control and FRSCC mixtures with 0.3% fiber ratio, and at 1.5% and 2% for FRSCC_0.6 and FRSCC_1 respectively, to obtain a targeted flow diameter of more than 600 mm for control mixture. Control and FRSCC compositions were prepared in a pan mixer with a capacity of 40 dm^3. Aggregate, cement and fly ash were first added to the mixer and mixed dry for 2 min. Then, water and SP additive were included and mixed for a further 3 min. Finally, fibers were added to the mixture and mixed for a further 2 min.

2.3. Testing procedures

After mixing, the fresh concrete experiments were carried out according to their relevant standards [46–48]. These included slump-flow diameter (mm) and related T_{500} time (s) and L-box test and resulted T_{200} and T_{400} times (s) and passing ability values (H_2/H_1). Several 100 × 100 × 100 mm cubes and 100 × 100 × 350 mm prisms were casted from each mixture to determine the compres-

Table 1
Physical and mechanical properties of all the fibers.

Type of Fiber	Length (mm)	Diameter (mm)	Aspect Ratio (Length/ Diameter)	Tensile Strength (MPa)	Specific Gravity	Elastic Modulus (MPa)	Melting Point (°C)
Steel	60	0.9	67	1100	7.85	200,000	1539
Polypropylene	40	0.75	53	338	0.91	4800	160
Polyamide	54	0.55	98	900	1.14	6800	256

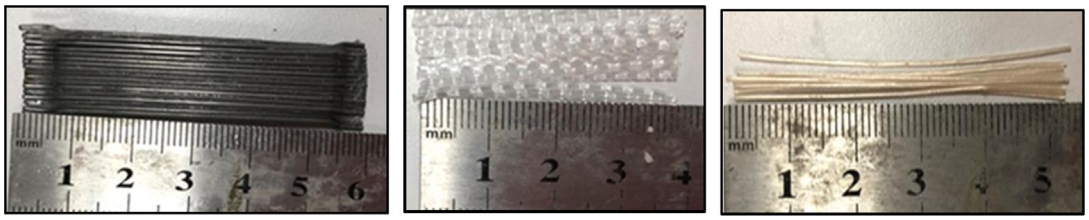

Fig. 1. Views of fibers used in this study a) ST b) PP c) PA.

Table 2
Mix-design of the control and FRSCC mixes.

Mixes	Cement (kg/m^3)	Fly Ash (kg/m^3)	Fine Aggregate (kg/m^3)	Coarse Aggregate (kg/m^3)	W/C	SP (%)	Fiber (%)
Control	375	125	930	670	0.48	1	–
STFRSCC_0.3	375	125	930	670	0.48	1	0.3
PPFRSCC_0.3	375	125	930	670	0.48	1	0.3
PAFRSCC_0.3	375	125	930	670	0.48	1	0.3
STFRSCC_0.6	375	125	930	670	0.48	1.50	0.6
PPFRSCC_0.6	375	125	930	670	0.48	1.50	0.6
PAFRSCC_0.6	375	125	930	670	0.48	1.50	0.6
STFRSCC_1	375	125	930	670	0.48	2	1.0
PPFRSCC_1	375	125	930	670	0.48	2	1.0
PAFRSCC_1	375	125	930	670	0.48	2	1.0

sive and flexural strengths as per ASTM C39/C39M and ASTM C 1018, respectively [49,50]. Compressive and flexural strength tests were conducted using UTC-4731 and UTC-5542 UTEST-brand automatic concrete compression and flexure testing machine, respectively. All specimens were left in a curing room at 22 ± 1 ℃ up to 28th days. At 28-day, three specimens of each SCC were dried in an oven at 100 ± 5 ℃ for 24 h, and then exposed to 2-hours high temperatures of 300, 500 and 800 ℃ in a 1250 °C capacity Protherm-brand furnace. The specimens were kept in a closed furnace after the 2 h exposure time until reaching a room temperature of around 23 °C. Then, the residual compressive (RCS) and flexural strengths (RSF) and toughness indices (TI) were determined and compared to the results of specimens not subjected to high temperatures. RCS and RFS were obtained by averaging the results of three tested specimens from each composition. TI, residual strength factors (RSF) and residual toughness (RT) capacities were obtained by testing three beam specimens of each SCC under three-point bending-loading machine, as per ASTM C1018 standard. The load–deflection curves of the beams were obtained automatically by a data acquisition system. The representative load–deflection graph of FRSCC specimens according to ASTM C1018 standard is given in Fig. 2.

According to ASTM C 1018, three toughness indices (TI) namely I_5, I_{10} and I_{20} are used to define the elastic–plastic behavior of concrete up to the selected displacement values (δ, 3δ, 5.5δ and 10.5δ) and residual strength factors (RSF) $R_{5,10} = 20*(I_{10}-I_5)$ and $R_{10,20} = 10*(I_{20}-I_{10})$ are calculated with regard to TI values. However, in order to eliminate the shortcoming of ASTM C1018 in regard to the visual determination of the first crack occurrence, the value corresponding to 85% of the first peak load in each curve was selected as first-crack point (δ). RT capacity calculated at (δ) is considered as a pre-peak RT capacity, while the sum of RT capacities calculated at 3δ, 5.5δ and 10.5δ is accepted as a post-peak RT capacity.

Microstructural characterization was also performed before and after subjecting each FRSCC to elevated temperatures. Analysis was completed using a high-performance scanning electron microscopy (SEM) machine (Carl Zeiss Ultra Plus FESEM), with a voltage acceleration of 20 kV and a resolution of 3.0 nm.

3. Experimental results

3.1. Fresh properties

The test results of fresh properties of control and FRSCC mixes are given in Table 3. While slump-flow value of the control concrete is around 670 mm, the FRSCC mixtures presented lower values of between 550 mm and 650 mm. The use of all fiber types at 0.3% content seems not affected the slump-flow diameter of FRSCCs compared to control-SCC (less than 5% differences). However, the results slightly reduced at 0.6 and 1% concentrations, with reductions of 9% and 13.4% for STFRSCC, 5.2% and 9% for PPFRSCC and 8.2 and 11.9% for PAFRSCC respectively. Thus, the incorporation of PA instead of ST appeared to slightly increase the flow of FRSCCs, though PP presented the greatest flow diameters than ST and PA. However, all FRSCCs displayed appropriate filling abilities for standard SCC compositions, which fall within the range of 550–650 mm according to class SF1 of EFNARC standard. Similarly, compared to the control SCC, the important delays in T_{500} time were

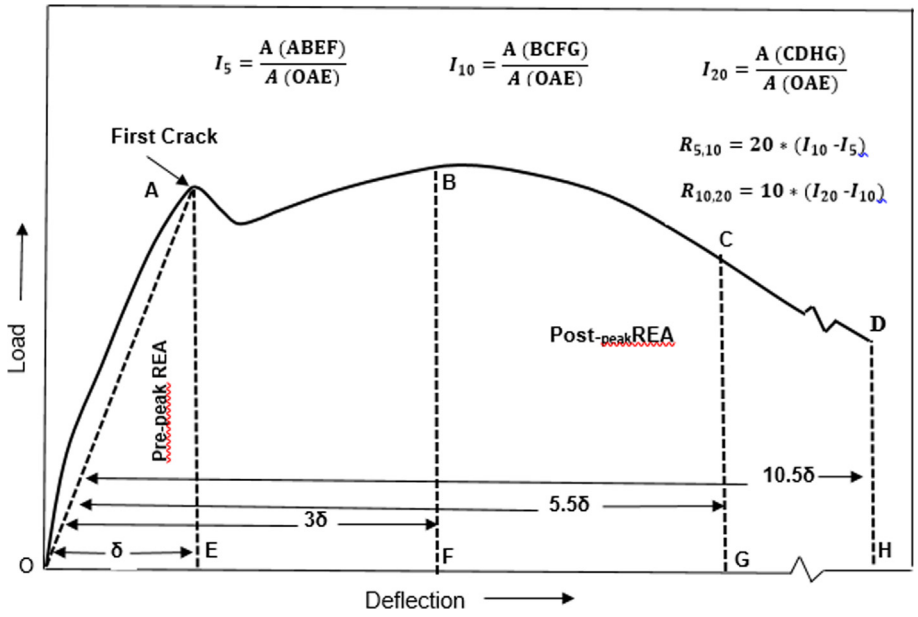

Fig. 2. Representative load–deflection graph of FRSCC specimens according to ASTM C1018 standard.

Table 3
Values for fresh properties of control and FRSCC mixes.

Mixes	Slump flow		L-box		
	Slump flow (mm)	T_{500} (s)	T_{200} (s)	T_{400} (s)	H_2/H_1
Control	670	5.3	3.6	6.1	0.93
PPFRSCC_0.3	660	7.1	5.3	8.2	0.89
PAFRSCC_0.3	650	7.6	7.4	12.9	0.87
STFRSCC_0.3	640	7.8	12.8	16.4	0.85
PPFRSCC_0.6	635	8.7	7.3	11.8	0.87
PAFRSCC_0.6	615	9.4	11.9	17.4	0.85
STFRSCC_0.6	610	10.2	15.5	22.8	0.83
PPFRSCC_1	610	10.1	11.6	14.1	0.84
PAFRSCC_1	590	11.7	13.4	18.9	0.83
STFRSCC_1	580	13.6	18.9	26.7	0.8

registered at higher fiber contents. Furthermore, PAFRSCCs showed lower T_{500} than STFRSCCs and slightly higher than PPFRSCCs, though all T_{500} values were in the same class of viscosity VS2 > 2S. Concerning the L-box results, T_{200} and T_{400} of PPFRSCC mixes have also lower values than STFRSCC and PAFRSCC compositions. In addition, while H_2/H_1 ratio was obtained as 0.93 for the control SCC, it reduced with increased fiber contents to be at 0.84–0.89 for PPFRSCC, 0.83–0.87 for PAFRSCC, and 0.8–0.85 for STFRSCC mixes. Thus, the prepared PP-, PA- and ST-based FRSCC mixtures fulfilled the obligation of a minimum cross-section filling ability of ≥0.8, as per the EFNARC standard. The greater fresh properties of PPSCCs than STSCCs can be explained by the fact that PP fibers are slithtly shorter and their geometric shape is more convenient compared to the hooked ST fibers, especially in the transition and progression stages of mixing. In addition, PA fibers were shown with higher water absorption capacity than PP [51,52], in line with their effects on the slump flow and L-box results.

3.2. Mass change of hardened concrete samples

The mass loss of control and FRSCC specimens was measured at high temperatures of both cube and prismatic beam samples. The average mass loss of each SCC composition is presented in Fig. 3. The mass losses of control and FRSCC specimens were less than 3.4% at 300 ℃, and slightly increased to be at the ranges of 7–8.5% and 10.5–13.6% at 500 °C and 800 °C, respectively. When compared to the control mix, the influence of PA fibers on the results was almost insignificant, particularly at temperatures of 500 and 800 °C. This effect was equivalent to that of PP and presented maximum mass loss reductions of less than 3.5% at the same high temperatures. Whereas the use of ST caused the mass loss to decrease noticeably with increased fiber and temperatures to reach up to 22.2% at 800 °C compared to the control SCC. The diverse effect of macro ST compared to macro PP and PA fibers can be related to the higher specific gravity of steel fibers, which may have partially compensated the mass loss of FRSCCs at advanced microstructural water evaporation and decomposition of hydration products [53]. Furthermore, the networks left from the melting of PA and PP fibers may have generated more water vapor [54], causing larger mass losses in PPFRSCC and PAFRSCC than ST-based mixes. It is worth mentioning that the endothermic response of macro PA and PP fibers looks comparable to the micro-PP fiber in term of mass loss presented in the literature to generate little differences when used in high performance concrete at 600 °C [16].

3.3. Residual compressive strengths

Fig. 4 shows the effect of ST, PP and PA fibers on the compressive strength results of different SCCs subjected to ambient and high temperatures. Table 4 presents the relative loss of compres-

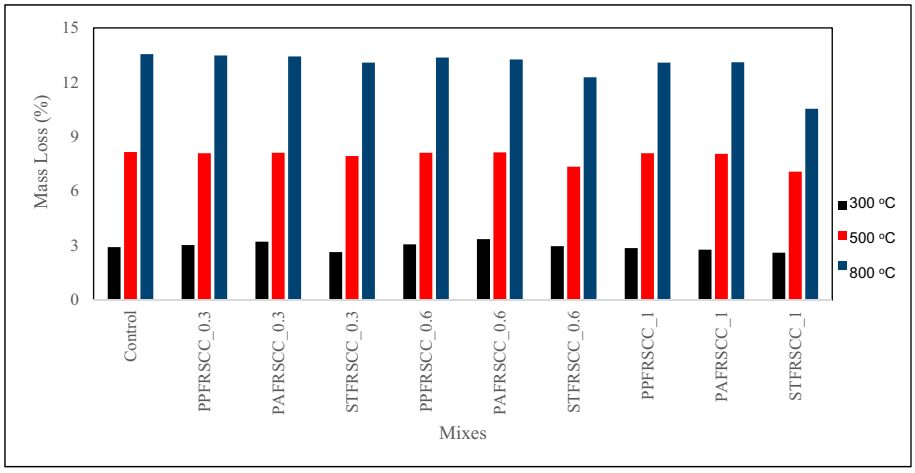

Fig. 3. Variation of mass loss for control and FRSCC specimens.

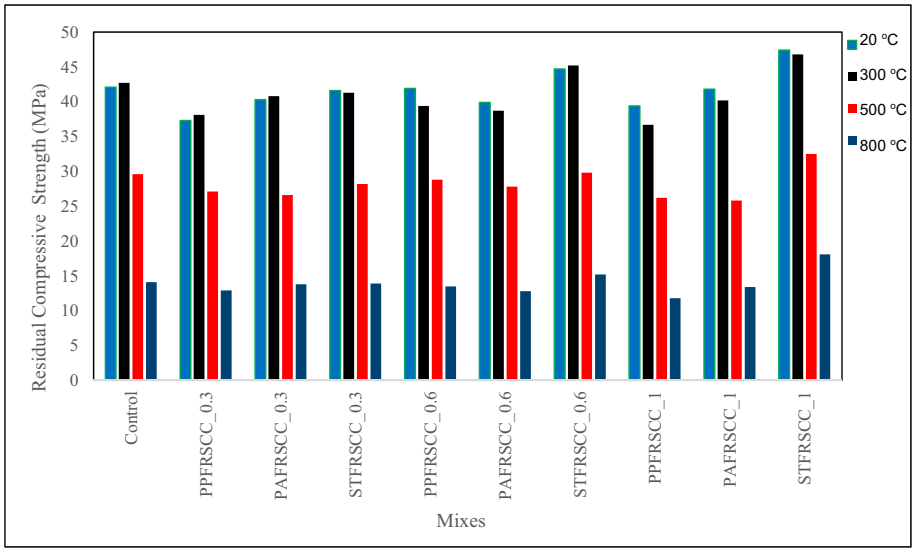

Fig. 4. Variation of compressive strengths in control and FRSSC specimens.

Table 4
Values for residual compressive strength (RCS) of control and FRSCC mixes.

Mixes	Relative loss at 300 °C (%)	Relative loss at 500 °C (%)	Relative loss at 800 °C (%)
Control	−1.43	29.69	66.51
PPFRSCC_0.3	−2.14	27.35	65.42
PAFRSCC_0.3	−1.24	34.00	65.76
STFRSCC_0.3	0.72	32.21	66.59
PPFRSCC_0.6	5.97	31.26	67.78
PAFRSCC_0.6	3.01	30.33	67.92
STFRSCC_0.6	−1.12	33.33	66.00
PPFRSCC_1	6.85	33.50	70.05
PAFRSCC_1	3.83	38.28	67.94
STFRSCC_1	1.27	31.43	61.81

sive strengths after exposure of heating at elevated temperatures. By considering the results of ambient curing, the addition of macro PA fibers caused slight strength decreases between 0.7% and 5.2% at different contents. These reductions were lower than those of macro PP, which presented reductions in the range of 5.2%-11.4% at the same concentrations. Unlike PP and PA, the use of ST at ambient temperature resulted in small increases of 6.2% and 12.6% at 0.6 and 1% respectively. Thus, macro PA fibers have slightly better effects compared to macro PP and reduced influence than ST, though the limited changes suggests that all macro fibers have limited effect on the compressive strength of SCC up to its peak load. It is to mention that Eidan et al. [26] noticed that PP fibers with 12 mm length presented higher strength reduction of SCC than that of 6 mm and explained the results by the higher number of fibers at 6-mm length. This is not the case in this study as PA has higher length and specific gravity and presented greater strengths than PP. Therefore, the reason is more likely related to the original mechanical properties of fibers than their numbers, as the elastic modulus of ST, PP and PA were 200000, 4800 and 6800 MPa respectively. When the temperature increased to 300 ℃, it was observed that there was a slight effect on the compressive strengths of control and FRSCC specimens, with even small increase in specimens marked by (-) in Table 4. This situation can be related to the evaporation of most free and capillary water at 300 ℃, as the loss of strength under this temperature was explained by the internal microstructural pressure caused by the escaped water [55,56]. Contrary to this, when the temperature rises to 500 and 800 ℃, there is a significant decrease in the compressive strength of the control and all of the FRSCC specimens. The reason for the high relative strength loss is the deterioration of CH crystals and C-S-H gels, especially after 500 ℃ [29,56,57]. At max-

imum fiber content of 1%, the relative loss of control SCC was 29.69% and 66.51% at 500 and 800 °C, while these values were 33.5% and 61.81%, 38.28% and 67.94%, 31.4% and 70.05% for STFRSCC_1, PAFRSCC_1 and PPFRSCC_1 respectively. Based on these results, only ST fibers at 1% content that makes a 4.7% contribution to the RCS capacity of plain SCC, though the negative effect of macro-PP and PA was limited, especially at 800 °C. Considering the previous studies conducted in the literature, it is seen that the results are quite incompatible each other as well as with this study. For instance, Eidan et al. [26] depicted that 12 mm long PP fibers were more effective than those with 6 mm in increasing the RCS of SCC by 25% and 21% respectively. Sadrmomtazi et al. [27] revealed that adding 0.3% of 25 mm-ST fibers and combining them with fly ash maintained 24% and 47% respectively, of RCS in SCC compositions exposed to 600 °C. Ding et al. [28] stated that there was a 94% decrease in the relative RCS value of control SCC at 900 °C compared to room condition, and 89% and 91% decreases 15 mm PP- and 35 mm ST-incorporated SCCs. The reason was explained by the melting point of PP which can provide space for internal tension stresses and the higher tendency of ST in slowing the crack spreading at high temperatures. In contrary to these statements, Sideris et al. [25] stated that the use of PP fibers with the length of 6 and 12 mm does not provide any increase in the RCS capacities of control SCC. Also, Uysal [31], Al Qadi et al. [32], Rios et al. [33] used PP fibers with lengths of 20 mm, 19 mm and 24 mm respectively and specified that PP fibers cannot generate a positive contribution in the residual strengths of SCC. They revealed that PP fibers are ineffective in limiting transverse deformations compared to ST fibers at high temperatures due to the randomly distributed microchannels created at low melting temperatures of PP. Also, the internal vapor pressure which can develop in the hallow structure left by the melted fibers can reduce the RCS capacities of SCC. This study supports the reduced effect of both macro synthetic and hooked ST fibers on the RCS of SCC, though ST seems better maintained the relative strength loss at higher temperature of 800 °C.

3.4. Flexural behavior

3.4.1. Load-deflection curves

The load–deflection curves of control and FRSCC specimens under third-point bending is given in Fig. 5. Adding fibers to SCCs changed their semi-brittle behavior after the first peak load and contributed noticeably to their ductile behavior, with the higher effect registered at increased fiber contents. The load–deflection curves of the control specimens showed a sudden drop after the initial peak load. At 20 °C, the behavior of the specimens with 0.3% fiber ratio after the first peak load was more brittle compared to those with 0.6% and 1% fiber ratios and their load–deflection curves decreased to zero without making sufficient deformation. Only PAFRSCC at 1% fiber level and STFRSCC specimens with 0.6% and 1% fiber ratios showed strain-hardening behavior (double-peak) after the first peak load was exceeded. However, at elevated temperatures, all SCC specimens with and without fibers suffered from loss of stiffness, strength and ductility. Although, this deterioration was not very effective at 300 ℃, it becomes critical at 500 and 800 ℃, where the maximum load of control and FRSCCs with 0.3 and 0.6% fibers reduced from the range of 20–30 kN at 300 °C to lower than 20 kN and 10 kN at 500 and 800 ℃ respectively.

3.4.2. Residual flexural strengths

Fig. 6 presents the flexural strengths of control and FRSCC mixes at normal and high temperature exposures and Fig. 7 shows the visual state of tested samples with 1% fiber ratio under room and 800 °C conditions. In addition, Table 5 provides the relative flexural loss under elevated temperatures. At ambient curing, except at a concentration of 0.3%, all the added fibers generated flexural strength increments compared to the control SCC. Negligible differences of less than 3.2% were measured at 0.3% content of macro PP, PA and ST fibers compared to control concrete. However, at 0.6% and 1%, the added fibers were effective in improving the flexural strength of SCC, with the optimized results registered for ST. The higher fiber concentration presented the greater flexural strength increments of 26.6% for STFRSCC_1 and 15.2% for PPFRSCC_1 and PAFRSCC_1. This can be related to the macro-fiber type used, which is reported in the literature to postpone the unstable evolution of micro cracks and prevent the unrestrained cracks in cementitious composites; hence, flexural strengths slightly improved at peak load [58]. The effect of macro PA was equivalent to that of PP and slightly lower than ST, as maximum differences of 0.08% and 1.8% can be calculated between PP- and PA-SCCs and around 6% and 11% between PP- and ST-SCCs at 0.6 and 1% respectively. This explain that the presence of macro ST generated higher load carrying capacity of SCC and better homogeneity of fiber distribution, leading to enhanced cracking resistance at ST-binder interface [59]. Compared to ambient environment, although negligible flexural strength changes were recorded when the specimens were exposed to high temperature of 300 °C, there were significant reductions in the results of all SCC mixes at 500 and 800 ℃. This is in line with the important mass loss measured at very high temperatures of 500 and 800 °C, and can be also related to the water evaporation and possible breakdown of hydration products such as portlandite, thus leading to reduced structural integrity and decreased flexural strengths in all SCC specimens. When compared to control SCC, the positive effect of macro PP, PA and ST fibers on preserving the residual flexural strengths was generally noticed at higher fiber contents of 0.6% and 1%. For instance, at temperatures of 500 °C, the relative loss of flexural strengths reduced by 3.5% and 4.5% for PPFRSCC_0.6 and PPFRSCC_1, 3.9% and 4.4% for PAFRSCC_0.6 and PAFRSCC_1 and 4.5% and 6.1% for STFRSCC_0.6 and ST-FRSCC-1 respectively, compared to control SCC. Furthermore, at 800 °C, relative strength loss reductions increased up to 5.3% to 8.6% for ST-SCCs, while it decreased slightly for PP- and PA-SCCs. As for the mass losses at high temperatures, macro ST-based specimens showed higher residual flexural strengths at high temperatures than equivalent length PP and PA-SCCs. This describes better capacity of macro ST compared to macro PP and PA in preserving the flexural strengths of SCC. In the literature, Ding et al. [28] showed equivalent performance of 35 mm- length ST compared to micro 15 mm-length PP and their results revealed around 5% increment of residual strengths for both ST- and PP-SCCs at 600 °C, and less than 1.2% at 900 °C compared to the control SCC. The reason was explained by the enhanced heat transfer factor of ST fibers against the elevated effect of PP in reducing the vapor pressure with its low melting temperature. Also, Sadrmomtazi et al. [27], revealed higher residual strength of up to 9% of SCC prepared with two concentrations of 25 mm-ST fibers compared to the reference composition at temperature of 600 °C. Thus, in addition to their types, the size of fibers can be considered as an important factor that can influence the residual flexural strengths of SCCs at high temperatures. At 500 °C and 800 °C, the melted macro size PP and PA fibers may have generated larger porous networks than those acquired at micro size [60], which resulted in lower effect on the relative loss of SCC compared to ST. On the other hand, it seems that the type of PP and PA synthetic fibers has a limited effect on the residual flexural strengths, though PA presented slightly better performances than PP.

3.4.3. Residual toughness capacity

The values of flexural toughness, T_{pre} and T_{post} values, toughness indices (TI) and residual strength factors (RSF) obtained from testing the control and FRSCCs at 20 °C, 300 °C, 500 °C and 800 ℃ are

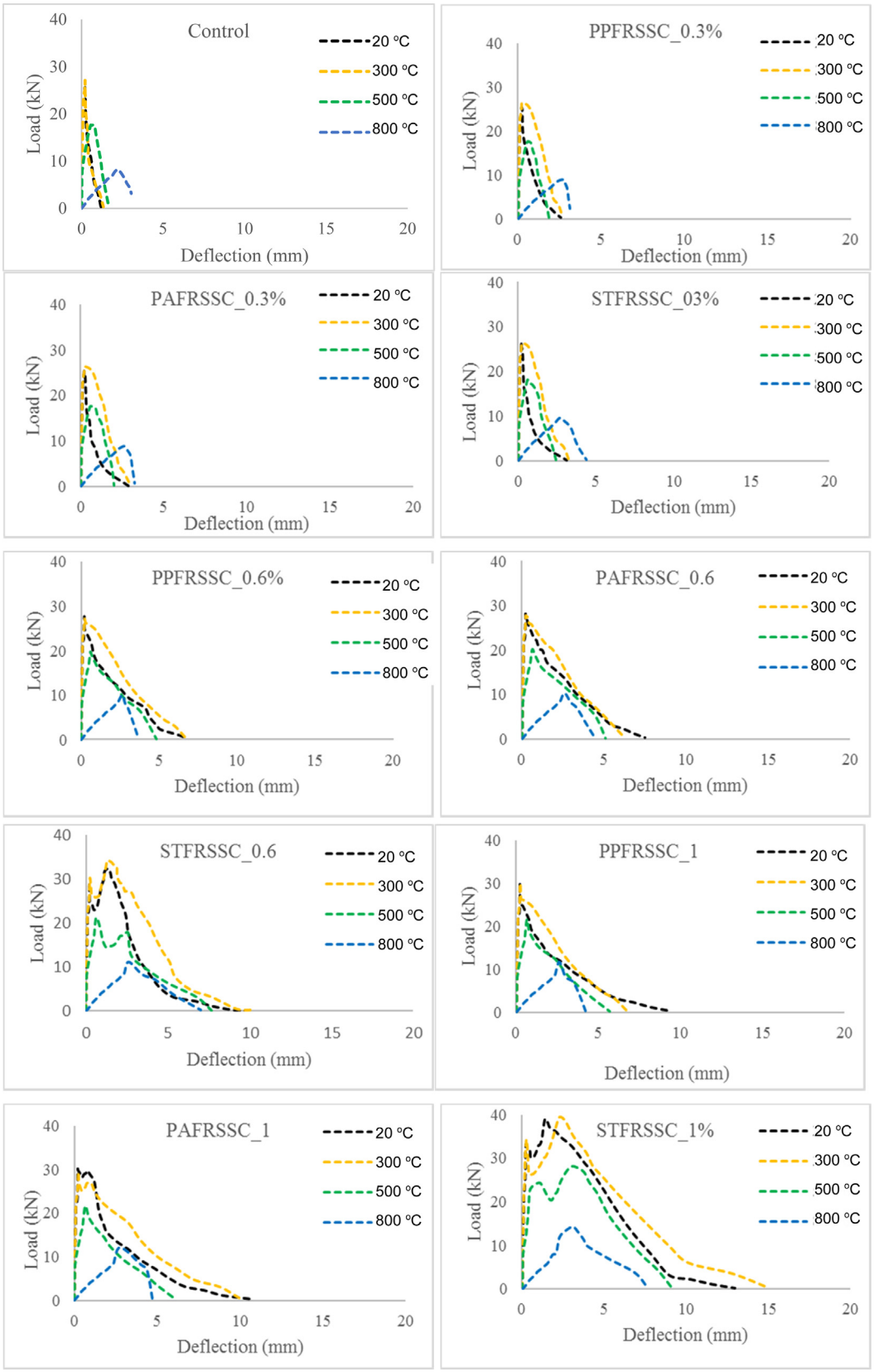

Fig. 5. Load-deflection graphs of control and FRSCC specimens.

given in Tables 6–9 respectively. As seen in Table 6, the post-peak RT increased significantly with increased macro PP, PA and ST fiber contents from 0 to 1%. In line with the load–deflection curves of Fig. 5, which showed an increased ductile aspect with increased fiber contents after the first peak load was exceeded, the post-peak RT capacities enhanced considerably between the control

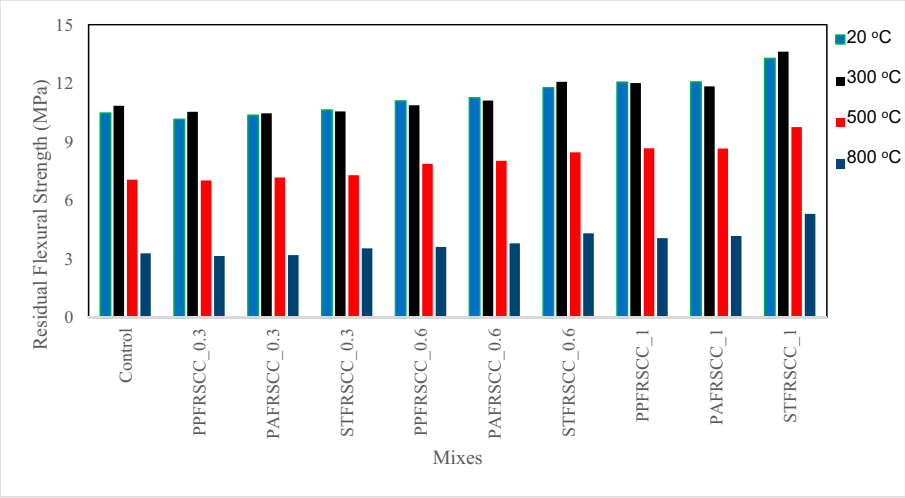

Fig. 6. Variation of flexural strengths in control and FRSSC specimens.

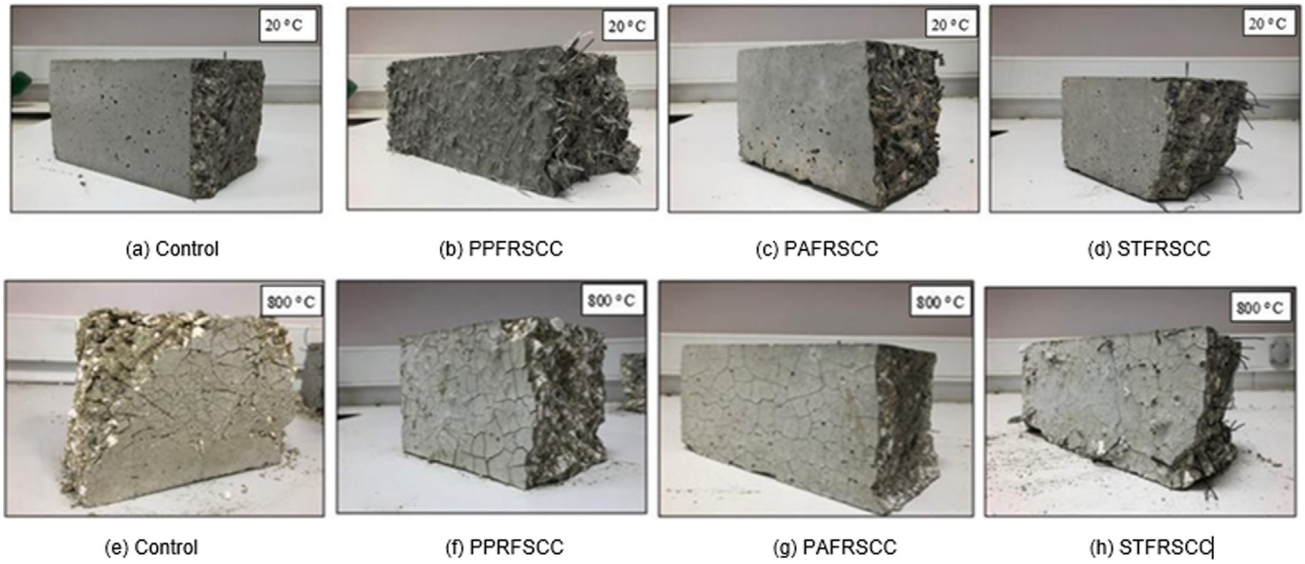

Fig. 7. The view of the control and FRSCC specimens at room temperature and after exposure to elevated temperatures.

Table 5
Values for residual flexural strength of control and FRSCC mixes.

Mixes	Relative loss at 300 °C (%)	Relative loss at 500 °C (%)	Relative loss at 800 °C (%)
Control	3.53	32.63	68.65
PPFRSCC_0.3	3.84	30.84	68.96
PAFRSCC_0.3	0.97	30.79	69.16
STFRSCC_0.3	−0.66	31.42	66.72
PPFRSCC_0.6	−2.07	29.10	67.48
PAFRSCC_0.6	−1.33	28.69	66.28
STFRSCC_0.6	2.63	28.12	63.35
PPFRSCC_1	−0.41	28.11	66.26
PAFRSCC_1	−1.91	28.25	65.38
STFRSCC_1	− 2.56	26.58	60.06

and 0.3%, 0.6% and 1% fiber concentrations. For example, at ambient curing, the post-peak of the control improved by 129% to 321%, 440% to 687% and 583% to 987% at 0.3%, 0.6% and 1% fiber contents, respectively. Comparatively, the pre-peak RT increments between the control and FRSCCs were relatively limited, at the ranges of −10% to 8.8%, 68% to 74% and 98% to 104% SCC, respectively. This reveals that macro PP, PA and ST fibers were not very effective in limiting the crack development and changing the behavior of SCC up to the first-peak load as compared to the great post-first peak effect. The influence of fibers on the pre-peak RT appears even reduced at higher temperature exposures. The reason for the different fiber effect between pre- and post-peak RT capacities is that, the macro PP, PA and ST fibers randomly distributed in the three dimensions (3D) of the SCC matrix may have intervened mostly in reducing the rapid and uncontrolled progression of cracks by showing bridging effects. This can be more effective after the formation of initial cracks and accordingly after the first peak load was exceeded [8,9,14,19]. Unlike the results of mass loss and flexural and compressive strengths where only small differences were registered between macro PP and PA fibers, the values of toughness, pre- and post-peak RT, TI and RSF of PAFRSCC specimens were remarkably higher than those of macro PPFRSCCs at the same fiber amount. This demonstrates that the greater tensile strength and elastic modulus of macro PA compared to PP were more effective in increasing the toughness properties of SCC than the other residual mechanical strengths. As for the previous test results, the advanced tensile strengths and elastic modulus of

Table 6
Toughness properties of at ambient curing

Mixes	Flexural Toughness (Nm)				Pre-peak RT (Nm)	Post-peak RT (Nm)	Toughness Indices (TI)			Residual Strength Factors (RSF)	
	δ	3δ	5,5δ	10,5δ			I_5	I_{10}	I_{20}	$R_{5,10}$	$R_{10,20}$
Control	2.49	6.12	8.84	–	2.49	14.96	2.46	3.55	–	21.85	
PPFRSCC_0.3	2.24	6.04	10.37	17.95	2.24	34.36	2.70	4.63	8.01	38.66	33.84
PAFRSCC_0.3	2.36	8.35	13.87	24.67	2.36	46.89	3.54	5.88	10.45	46.78	45.76
STFRSCC_0.3	2.71	11.63	18.55	32.87	2.71	63.05	4.29	6.85	12.13	51.07	52.84
PPFRSCC_0.6	4.18	12.85	23.76	44.11	4.18	80.72	3.07	5.68	10.55	52.20	48.68
PAFRSCC_0.6	4.25	14.46	28.84	52.15	4.25	95.45	3.40	6.79	12.27	67.67	54.85
STFRSCC_0.6	4.34	19.19	35.23	63.34	4.34	117.76	4.42	8.12	14.59	73.92	64.77
PPFRSCC_1	4.94	17.26	30.92	53.95	4.94	102.13	3.49	6.26	10.92	55.30	46.62
PAFRSCC_1	5.02	20.15	38.21	75.87	5.02	134.23	4.01	7.61	15.11	71.95	75.02
STFRSCC_1	5.09	24.78	48.92	88.89	5.09	162.59	4.87	9.61	17.46	94.85	78.53

Table 7
Toughness properties of at ambient curing at 300 °C

Mixes	Flexural Toughness (Nm)				Pre-peak RT (Nm)	Post-peak RT (Nm)	Toughness Indices (TI)			Residual Strength Factors (RSF)	
	δ	3δ	5,5δ	10,5δ			I_5	I_{10}	I_{20}	$R_{5,10}$	$R_{10,20}$
Control	2.73	7.85	12.46	–	2.73	20.31	2.88	4.56	–	33.77	–
PPFRSCC_0.3	2.63	9.23	17.18	25.32	2.63	51.73	3.51	6.53	9.63	60.46	30.95
PAFRSCC_0.3	2.59	10.59	20.51	32.66	2.59	63.76	4.09	7.92	12.61	76.6	46.91
STFRSCC_0.3	2.66	13.88	25.58	40.89	2.66	80.35	5.22	9.62	15.37	87.97	57.56
PPFRSCC_0.6	3.96	15.02	26.99	48.94	3.96	90.95	3.79	6.82	12.36	60.45	55.43
PAFRSCC_0.6	4.08	18.65	33.87	60.89	4.08	113.41	4.57	8.3	14.92	74.61	66.23
STFRSCC_0.6	4.21	23.14	42.81	74.08	4.21	140.03	5.5	10.17	17.6	93.44	74.28
PPFRSCC_1	4.82	18.82	33.15	58.41	4.82	110.38	3.9	6.88	12.12	59.46	52.41
PAFRSCC_1	4.74	20.34	43.15	73.21	4.74	136.7	4.29	9.1	15.45	96.24	63.42
STFRSCC_1	5.14	27.66	54.75	96.56	5.14	178.97	5.38	10.65	18.79	105.41	81.34

Table 8
Toughness properties of at ambient curing at 500 °C

Mixes	Flexural Toughness (Nm)				Pre-peak RT (Nm)	Post-peak RT (Nm)	Toughness Indices (TI)			Residual Strength Factors (RSF)	
	δ	3δ	5,5δ	10,5δ			I_5	I_{10}	I_{20}	$R_{5,10}$	$R_{10,20}$
Control	2.37	5.95	–	–	2.37	5.95	2.51	–	–	–	–
PPFRSCC_0.3	2.32	6.32	–	–	2.32	6.32	2.72	–	–	–	–
PAFRSCC_0.3	2.41	7.64	–	–	2.41	7.64	3.17	–	–	–	–
STFRSCC_0.3	2.86	9.47	–	–	2.86	9.47	3.31	–	–	–	–
PPFRSCC_0.6	3.11	8.86	14.43	–	3.11	23.29	2.85	4.64	–	–	–
PAFRSCC_0.6	3.31	11.26	18.79	–	3.31	30.05	3.4	5.68	–	–	–
STFRSCC_0.6	3.42	14.61	25.59	38.86	3.42	79.06	4.27	7.48	11.36	64.21	38.8
PPFRSCC_1	3.64	10.46	17.42	–	3.64	27.88	2.87	4.79	0	–	–
PAFRSCC_1	3.51	14.67	23.68	–	3.51	38.35	4.18	6.75	0	–	–
STFRSCC_1	3.94	20.78	35.87	56.97	3.94	113.62	5.27	9.1	14.46	76.6	53.55

Table 9
Toughness properties of at ambient curing at 800 °C

Mixes	Flexural Toughness (Nm)				Pre-peak RT (Nm)	Post-peak RT (Nm)	Toughness Indices (TI)			Residual Strength Factors (RSF)	
	δ	3δ	5,5δ	10,5δ			I_5	I_{10}	I_{20}	$R_{5,10}$	$R_{10,20}$
Control	1.64	–	–	–	1.64	–	–	–	–	–	–
PPFRSCC_0.3	1.81	–	–	–	1.81	–	–	–	–	–	–
PAFRSCC_0.3	1.93	–	–	–	1.93	–	–	–	–	–	–
STFRSCC_0.3	2.27	–	–	–	2.27	–	–	–	–	–	–
PPFRSCC_0.6	2.09	–	–	–	2.09	–	–	–	–	–	–
PAFRSCC_0.6	2.26	–	–	–	2.26	–	–	–	–	–	–
STFRSCC_0.6	2.48	6.82	–	–	2.48	6.82	3.02	–	–	–	–
PPFRSCC_1	2.59	–	–	–	2.59	–	–	–	–	–	–
PAFRSCC_1	2.68	–	–	–	2.68	–	–	–	–	–	–
STFRSCC_1	3.14	12.94	–	–	3.14	12.94	4.83	–	–	–	–

macro ST compared to PA and PP fibers caused the toughness performance of macro STFRSCCs to significantly increase compared to those of PPFRSCCs and PAFRSCCs with the same fiber content. Besides, the hooked geometrical shape of ST may have created better fiber-friction response and longer time to strip the fibers from the SCC matrix due to the plastic deformation of the hook [61]. This explanation is also supported by the extra RT capacities generated in ST- than PA and PP- based SCCs, especially at post-peak stage where the STFRSCCs presented 46% to 84% higher residual toughness than PPFRSCCs and 21% to 35% compared to PAFRSCCs at ambient environment. From Table 7, when the temperature raised to 300 °C, except some pre-peak RT values of the control, PPFRSCC_0.3 and PAFRSCC_0.3 which showed reduction compared to room curing, post-peak RT, TI and RSF capacities of control and all FRSCC specimens increased, though with different extents. However, the enhancements in the toughness parameters reduced with increased fiber contents to reach differences of less than 10% at 1% ST, PP and PA fibers. These results are in line with some previous studies which also presented a reduced effect or even small improvements of the post-peak performance of SCC at 300 °C [30]. In addition to the effect of ST fiber and melted macro PA and PP, the additional hydration and pozzolanic reaction of cement and fly ash may have accelerated at this temperature, leading to a partial or complete compensation of the randomly distributed voids created from the evaporated water and reducing the effect of high temperatures up to certain limit [27,62]. Another remark is related to the effect of macro PP and PA fibers at 0.3% concentration, which they revealed higher post-peak RT capacity than ST-specimens, in contrary to the results of 0.6% and 1% fiber contents. Thus, at 0.3%, the melted macro PP and PA fibers helped better the post-peak RT, likely by creating optimized spaces to increase the cement and fly ash reaction and related interfacial bond [63]. It is worth mentioning that Sadrmomtazi et al al. [27] and Ding et al. [28] found that both ST and micro PP fibers were not effective in increasing the toughness performance of SCC at higher temperatures between 200 and 300 °C. This highlights again the high influence of fiber geometry and contents on the residual performance of cementitious materials at elevated temperatures. However, when the temperatures raised to 500 °C and 800 °C, the pre-peak RT, post-peak RT, TI and RSF capacities of control and FRSCC specimens decreased noticeably. For instance, at 800 ℃, the post-peak RT was not obtained for the control, PPFRSCC and PAFRSCC specimens; while STFRSCCs endured decreases of 94.2% and 92.04% at 0.6% and 1% ST contents respectively. Also, while the toughness capacity up to 10.5δ deflection point was obtained in FRSCC specimens at room and 300 ℃ temperatures, this measurement was available only for STFRSCC_0.6 and STFRSCC_1 at 500 ℃, and at 800 ℃, even the post-peak RT capacities of STFRSCC_0.6 and STFRSCC_1 was not achieved up to 3δ deflection point. At high temperatures of 500 °C and 800 °C, the contribution of the melted macro PA and PP up to 10.5δ and 3δ points respectively, was much lower than that of ST fibers of various amounts. Thus, the post-peak RT capacities, RSF and some TI of PPFRSCCs and PAFRSCCs were not obtained at 10.5δ and 3δ points. Furthermore, the available values of toughness and TI were with similar trends and small differences at 500 °C and 800 °C. As the melting points of macro PA and PP fibers are about 256 °C and 160 ℃ respectively, there are less chance for these fibers to help retaining

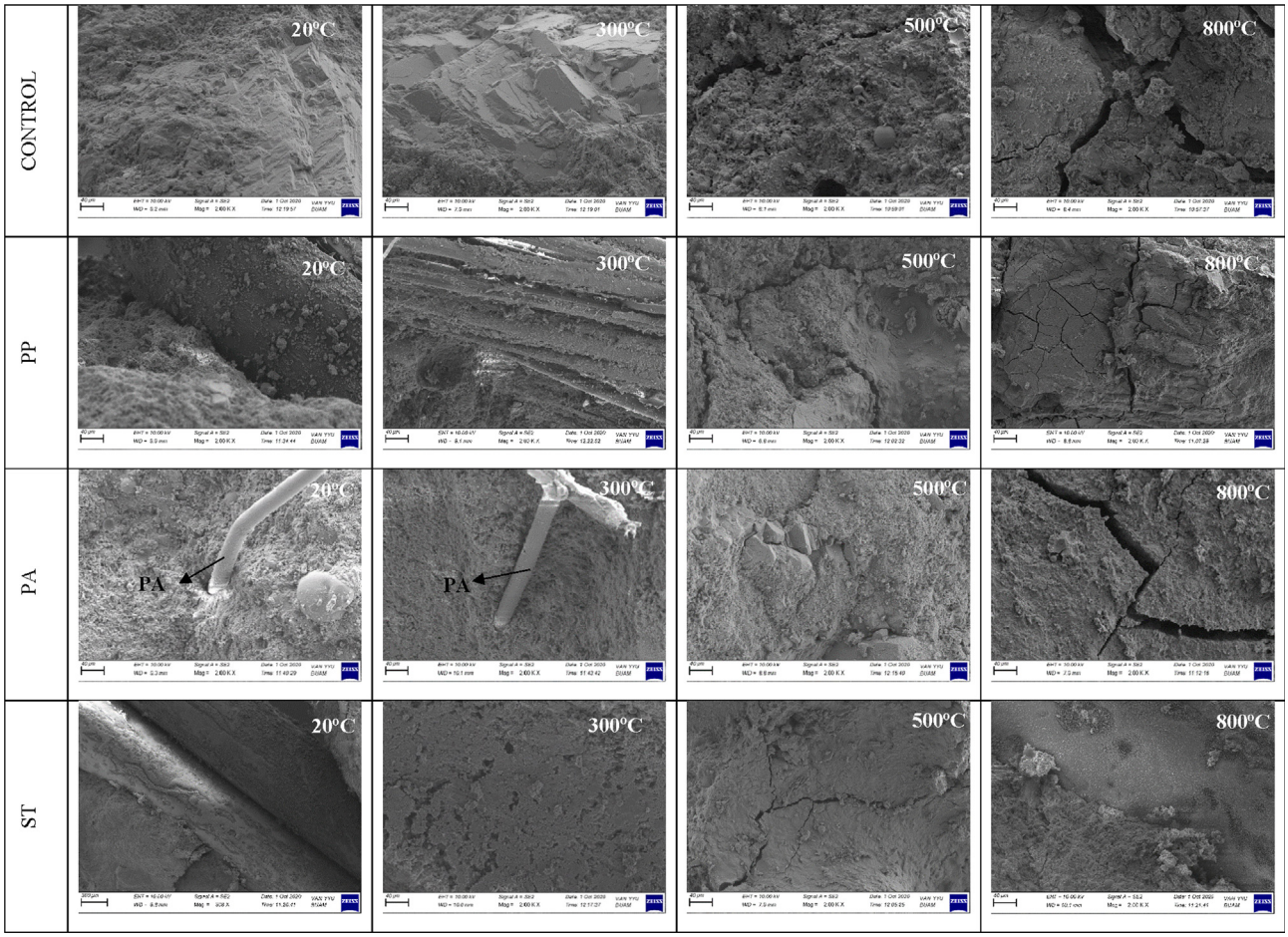

Fig. 8. SEM images of control and FRSCCs at normal and high temperatures.

the integrity of SCC specimens at higher temperatures of 500 and 800 ℃, especially with their important length [26]. Since the melting point of ST fibers is about 1538 ℃, less deterioration occurred in their physical and mechanical properties at high temperatures, which relatively helped maintaining the integrity of SCC [64,65].

4. SEM analysis

The SEM images of control, PPFRSCC_1, PAFRSCC_1 and STFRSCC_1 exposed to different elevated temperatures are presented in Fig. 8. The control and FRSCC samples exhibited different extents of microstructural deterioration when increased temperatures were applied. Also, microcracks were expanded and turned into larger macro-sized formations and more physical integrity losses were pronounced, especially at 500 and 800 °C. At 300 °C, dense cement matrix was noticed in all SCCs and some PP and PA fibers were still available, though the temperature exceeded their melting points. The remaining macro PA and PP fibers can be seen partly broken while forming a solid bond with the surrounded cement matrix, which confirm the previous explanation about the possible filling effect of the porous fiber–matrix interface with hydration products. According to Tai et al [66], the vaporized water can stimulate the reaction of cementitious materials up to 400 °C temperature, leading to more coherent and strong structure [27]. The use of high amount of fly ash in the SCC compositions may have also provided an additional source for the development of C-S-H products at 300 °C, as this was shown even to decrease the risk of cracking at temperatures under 600 °C [67]. Thus, the important growth of reaction products and related stronger microstructure may have helped protecting some macro PP and PA fibers and increasing the bond of ST fibers at 300 °C, in line with the residual flexural strengths and toughness capacity results at this temperature. At 500 °C and 800 °C, the high thermal stress and the evaporation of the micro-retained water influenced negatively the integrity of the formed reaction products, which weakened some areas in the cement matrix and led to the initiation and increase of cracks [68]. This effect was noticed more clearly in the SEM images of the control SCC compared to those of FRSCC specimens at 500 °C and 800 °C. However, the complete melting of macro PP and PA fibers seem unenabled them to transfer the stresses from the weak to the robust sections and consequently some macro cracks were also developed in the microstructure of PPFRSCC and PAFRSCC. The denser microstructure of the macro-PP and PA-based specimens compared to the control SCC can be related to the fact that part of the internal thermal pressure may have been mitigated through the created spaces from the melted fibers. Nevertheless, the hooked macro ST in STFRSCC looks partially preserved its bridging function by limiting the expanded cracks more effectively compared to PP and PA, consequently larger and higher number of macro-cracks were engendered in the microstructure of PPFRSCC and PAFRSCC than STFRSCC.

5. Conclusions

This paper considered the effect of macro-sized polypropylene (PP), polyamide (PA) and steel (ST) fibers on the residual physical and mechanical performance of fiber reinforced self-compacting concretes (FRSCC). The temperatures studied were 20 °C, 300 °C, 500 °C and 800 °C. The results obtained from the experimental program are summarized as follows.

- The incorporation of macro-ST fibers caused higher reductions in the fresh properties than PP and PA with equivalent length and concentration. Also, the more convenient geometric shape and absorption capacity of macro PP resulted in lower negative effect on the workability measurements compared to PA and ST fibers, though the standard SCC ranges were reached up to 1% of all fibers.
- At the same fiber content, macro PA presented comparable performance than PP and generated insignificant changes in the mass loss of SCC under high temperatures. Whereas ST caused the mass loss to decrease noticeably up to 22.2% at 800 °C.
- Only ST fibers at 1% content that made a small positive contribution to the residual compressive strength capacity under normal and high temperatures, and macro-PP and PA showed even slightly higher relative strength loss than the control SCC, especially at 500 °C.
- The positive effect of macro ST fibers on preserving the residual flexural strengths of SCC was noticed particularly at maximum temperature of 800 °C, though PP and PA also resulted in slight improvements with increased fiber contents.
- Unlike the results of mass loss and compressive and flexural strengths, macro PA-specimens exhibited clear higher toughness parameters than those of macro PP at ambient environment. Also, at 300 °C, macro PA and PP fibers at 0.3% concentration generated higher post-peak residual toughness capacity than ST-specimens. However, ST fibers were much more effective in increasing the residual toughness parameters at high temperatures of 500 °C and 800 °C where PA and PP were completely melted.
- SEM images confirmed the denser microstructure of all SCC specimens at 300 °C compared to ambient environment, though cracks with different extents were developed and extended at higher temperatures. In contrary to macro PA and PP which were not able to mitigate the developed cracks, the hooked macro ST helped limiting the expanded cracks at advanced temperatures of 500 °C and 800 °C.

Declaration of Competing Interest

The authors declare that they have no known competing financial interests or personal relationships that could have appeared to influence the work reported in this paper.

Acknowledgement

This study was supported by the Department of Scientific Research Projects of University of Van Yüzüncü Yıl, Van, Turkey with the project ID 5792.

References

[1] K. Ozawa, K. Maekawa, H. Okamura, 1990, May. High performance concrete with high filling capacity. In Admixtures for Concrete-Improvement of Properties: Proceedings of the International RILEM Symposium (Vol. 5, p. 60). CRC Press.
[2] H. Okamura, K. Ozawa, M. Ouchi, Self-compacting concrete, Struct. Concr. 1 (1) (2000) 3–17.
[3] A. Kefelegn, A. Gebre, Performance of self-compacting concrete used in congested reinforcement structural element, Eng. Struct. 214 (2020) 110665, https://doi.org/10.1016/j.engstruct.2020.110665.
[4] K.N. Rahal, A.L. Khaleefi, A. Al-Sanee, An experimental investigation of shear-transfer strength of normal and high strength self compacting concrete, Eng. Struct. 109 (2016) 16–25, https://doi.org/10.1016/j.engstruct.2015.11.015.
[5] I.M. Belmonte, F.J. Benito Saorin, C.P. Costa, M.V. Paya, Quality of the surface finish of self-compacting concrete, J. Build. Eng. 28 (2020) 101068, https://doi.org/10.1016/j.jobe.2019.101068.
[6] N. Singh, P. Kumar, P. Goyal, Reviewing the behaviour of high volume fly ash based self compacting concrete, J. Build. Eng. 26 (2019) 100882, https://doi.org/10.1016/j.jobe.2019.100882.
[7] M. Benaicha, A. Belcaid, A.H. Alaoui, O. Jalbaud, Y. Burtschell, Evolution of pressure generated by self compacting concrete on a vertical channel, Eng. Struct. 191 (2019) 432–438, https://doi.org/10.1016/j.engstruct.2019.04.079.

[8] M. Hsie, C. Tu, P.S. Song, Mechanical properties of polypropylene hybrid fiber-reinforced concrete, Mater. Sci. Eng., A 494 (1–2) (2008) 153–157, https://doi.org/10.1016/j.msea.2008.05.037.
[9] M. Nili, V. Afroughsabet, The long-term compressive strength and durability properties of silica fume fiber-reinforced concrete, Mater. Sci. Eng., A 531 (2012) 107–111, https://doi.org/10.1016/j.msea.2011.10.042.
[10] Z. Sun, Q. Xu, Microscopic, physical and mechanical analysis of polypropylene fiber reinforced concrete, Mater. Sci. Eng., A 527 (1–2) (2009) 198–204, https://doi.org/10.1016/j.msea.2009.07.056.
[11] Y. Jiang, L.H. Zhang, Q.F. Fang, T. Zhang, X.P. Wang, T. Hao, C.S. Liu, Toughness enhancement of tungsten reinforced with short tungsten fibres, Mater. Sci. Eng., A 690 (2017) 208–213, https://doi.org/10.1016/j.msea.2017.02.106.
[12] F. de Andrade Silva, B. Mobasher, R.D. Toledo Filho, Fatigue behavior of sisal fiber reinforced cement composites, Mater. Sci. Eng., A 527 (21–22) (2010) 5507–5513, https://doi.org/10.1016/j.msea.2010.05.007.
[13] A. Hassan, F. Khairallah, H. Mamdouh, M. Kamal, Structural behaviour of self-compacting concrete columns reinforced by steel and glass fibre-reinforced polymer rebars under eccentric loads, Eng. Struct. 188 (2019) 717–728, https://doi.org/10.1016/j.engstruct.2019.03.067.
[14] N. Buratti, C. Mazzotti, M. Savoia, Post-cracking behaviour of steel and macro-synthetic fibre-reinforced concretes, Constr. Build. Mater. 25 (5) (2011) 2713–2722, https://doi.org/10.1016/j.conbuildmat.2010.12.022.
[15] F. Aslani, S. Nejadi, Self-compacting concrete incorporating steel and polypropylene fibers: Compressive and tensile strengths, moduli of elasticity and rupture, compressive stress–strain curve, and energy dissipated under compression, Compos. B Eng. 53 (2013) 121–133, https://doi.org/10.1016/j.compositesb.2013.04.044.
[16] N. Banthia, F. Majdzadeh, J. Wu, V. Bindiganavile, Fiber synergy in Hybrid Fiber Reinforced Concrete (HyFRC) in flexure and direct shear, Cem. Concr. Compos. 48 (2014) 91–97, https://doi.org/10.1016/j.cemconcomp.2013.10.018.
[17] B. Li, Y. Chi, L. Xu, Y. Shi, C. Li, Experimental investigation on the flexural behavior of steel-polypropylene hybrid fiber reinforced concrete, Constr. Build. Mater. 191 (2018) 80–94, https://doi.org/10.1016/j.conbuildmat.2018.09.202.
[18] J.H. Lee, B. Cho, E. Choi, Y.H. Kim, Experimental study of the reinforcement effect of macro-type high strength polypropylene on the flexural capacity of concrete, Constr. Build. Mater. 126 (2016) 967–975, https://doi.org/10.1016/j.conbuildmat.2016.09.017.
[19] D.A.S. Rambo, F. de Andrade Silva, R.D. Toledo Filho, Mechanical behavior of hybrid steel-fiber self-consolidating concrete: materials and structural aspects, Mater. Des. 1980–2015 (54) (2014) 32–42, https://doi.org/10.1016/j.matdes.2013.08.014.
[20] F. Soltanzadeh, V.M. Cunha, J.A. Barros, Assessment of different methods for characterization and simulation of post-cracking behavior of self-compacting steel fiber reinforced concrete, Constr. Build. Mater. 227 (2019) 116704, https://doi.org/10.1016/j.conbuildmat.2019.116704.
[21] M. Pająk, J.J. Aniszewski, L. Kruszka, Laboratory investigation on the influence of high compressive strain rates on the hybrid fibre reinforced self-compacting concrete, Constr. Build. Mater. 2227 (2019), https://doi.org/10.1016/j.conbuildmat.2019.116704 116687.
[22] S. Widodo, Fresh and hardened properties of Polypropylene fiber added Self-Consolidating Concrete, Int. J. Civil Struct. Eng. 3 (1) (2012) 85, https://doi.org/10.6088/ijcser.201203013008.
[23] T. Ansari rad, J. Tanzadeh, A. pourdada, Laboratory evaluation of self-compacting fiber-reinforced concrete modified with hybrid of nanomaterials, Constr. Build. Mater. 232 (2020) 117211, https://doi.org/10.1016/j.conbuildmat.2019.117211.
[24] M.G. Alberti, A. Enfedaque, J.C. Gálvez, A. Cortez, Optimisation of fibre reinforcement with a combination strategy and through the use of self-compacting concrete, Constr. Build. Mater. 235 (2020) 117289, https://doi.org/10.1016/j.conbuildmat.2019.117289.
[25] K.K. Sideris, P. Manita, Residual mechanical characteristics and spalling resistance of fiber reinforced self-compacting concretes exposed to elevated temperatures, Constr. Build. Mater. 41 (2013) 296–302, https://doi.org/10.1016/j.conbuildmat.2012.11.093.
[26] J. Eidan, I. Rasoolan, A. Rezaeian, D. Poorveis, Residual mechanical properties of polypropylene fiber-reinforced concrete after heating, Constr. Build. Mater. 198 (2019) 195–206, https://doi.org/10.1016/j.conbuildmat.2018.11.209.
[27] A. Sadrmomtazi, S.H. Gashti, B. Tahmouresi, Residual strength and microstructure of fiber reinforced self-compacting concrete exposed to high temperatures, Constr. Build. Mater. 230 (2020) 116969, https://doi.org/10.1016/j.conbuildmat.2019.116969.
[28] Y. Ding, C. Azevedo, J.B. Aguiar, S. Jalali, Study on residual behaviour and flexural toughness of fibre cocktail reinforced self compacting high performance concrete after exposure to high temperature, Constr. Build. Mater. 26 (1) (2012) 21–31, https://doi.org/10.1016/j.conbuildmat.2011.04.058.
[29] C.K. Mahapatra, S.V. Barai, Temperature impact on residual properties of self-compacting based hybrid fiber reinforced concrete with fly ash and colloidal nano silica, Constr. Build. Mater. 198 (2019) 120–132, https://doi.org/10.1016/j.conbuildmat.2018.11.155.
[30] H. Xargay, P. Folino, L. Sambataro, G. Etse, Temperature effects on failure behavior of self-compacting high strength plain and fiber reinforced concrete, Constr. Build. Mater. 165 (2018) 723–734, https://doi.org/10.1016/j.conbuildmat.2017.12.137.
[31] M. Uysal, Self-compacting concrete incorporating filler additives: Performance at high temperatures, Constr. Build. Mater. 26 (1) (2012) 701–706, https://doi.org/10.1016/j.conbuildmat.2011.06.077.
[32] A.N. Al Qadi, S.M. Al-Zaidyeen, Effect of fibre content and specimen shape on residual strength of polypropylene fibre self-compacting concrete exposed to elevated temperatures, J. King Saud Univ.-Eng. Sci. 26 (1) (2014) 33–39, https://doi.org/10.1016/j.jksues.2012.12.002.
[33] J.D. Ríos, H. Cifuentes, C. Leiva, C. García, M.D. Alba, Behavior of high-strength polypropylene fiber-reinforced self-compacting concrete exposed to high temperatures, J. Mater. Civ. Eng. 30 (11) (2018) 04018271. https://orcid.org/0000-0001-6302-418X.
[34] A. Khajuria, K. Bohra, P. Balaguru, Long term durability of synthetic fibers in concrete, Special Publication 126 (1991) 851–868.
[35] P.S. Song, S. Hwang, B.C. Sheu, Strength properties of nylon-and polypropylene-fiber-reinforced concretes, Cem. Concr. Res. 35 (8) (2005) 1546–1550, https://doi.org/10.1016/j.cemconres.2004.06.033.
[36] J.K. Jeon, W. Kim, C.K. Jeon, J.C. Kim, Processing and mechanical properties of macro polyamide fiber reinforced concrete, Materials 7 (12) (2014) 7634–7652, https://doi.org/10.3390/ma7127634.
[37] J.K. Jeon, W. Kim, G.Y. Kim, C.K. Jeon, Polyamide fiber reinforced shotcrete for tunnel application, Materials 9 (3) (2016) 163, https://doi.org/10.3390/ma9030163.
[38] S. Guler, The effect of polyamide fibers on the strength and toughness properties of structural lightweight aggregate concrete, Constr. Build. Mater. 173 (2018) 394–402, https://doi.org/10.1016/j.conbuildmat.2018.03.212.
[39] H. Kim, G. Kim, S. Lee, M. Son, G. Choe, J. Nam, Strain rate effects on the compressive and tensile behavior of bundle-type polyamide fiber-reinforced cementitious composites, Compos. B Eng. 160 (2019) 50–65, https://doi.org/10.1016/j.compositesb.2018.10.008.
[40] H. Kim, G. Kim, N. Gucunski, J. Nam, J. Jeon, Assessment of flexural toughness and impact resistance of bundle-type polyamide fiber-reinforced concrete, Compos. B Eng. 78 (2015) 431–446, https://doi.org/10.1016/j.compositesb.2015.04.011.
[41] S.P. Yap, U.J. Alengaram, M.Z. Jumaat, Enhancement of mechanical properties in polypropylene–and nylon–fibre reinforced oil palm shell concrete, Mater. Des. 49 (2013) 1034–1041, https://doi.org/10.1016/j.matdes.2013.02.070.
[42] A. Çavdar, Investigation of freeze–thaw effects on mechanical properties of fiber reinforced cement mortars, Compos. B Eng. 58 (2014) 463–472, https://doi.org/10.1016/j.compositesb.2013.11.013.
[43] T.K. Tran, N.T. Tran, Klm, D.J.,, Enhancing impact resistance of hybrid ultra-high-performance fiber-reinforced concretes through strategic use of polyamide fibers, Constr. Build. Mater. 271 (2021), https://doi.org/10.1016/j.conbuildmat.2020.121562 121562.
[44] T.S. En Cement- Stage 1: General cements – component 197–1:2012. TSE, Ankara Turkey
[45] EFNARC, 2005. The European Guidelines for Self-Compacting Concrete, Specification, Production and Use the Self Compacting Concrete European Project Group, Warrington, 68.
[46] EN 12350-8:2010, Testing fresh concrete. Self-compacting concrete. Slump-flow test.
[47] EN 12350-9:2010, Testing fresh concrete. Self-compacting concrete. V funnel test.
[48] EN 12350-10:2010, Testing fresh concrete. Self-compacting concrete. L-box test.
[49] ASTM C39/C39M-18:2018. Standard Test Method for Compressive Strength of Cylindrical Concrete Specimens; ASTM International: West Conshohocken, PA, USA.
[50] ASTM C 1018-97:1992, Standard test method for flexural toughness and first-crack strength of fiber- reinforced concrete (using ream with third-point loading). Annual Book of ASTM Standards, ASTM Committee C-9(1992)514-520,1997.
[51] L. Monson, M. Braunwarth, C.W. Extrand, Moisture absorption by various polyamides and their associated dimensional changes, J. Appl. Polym. Sci. 107 (1) (2008) 355–363, https://doi.org/10.1002/(ISSN)1097-462810.1002/app.v107:110.1002/app.27057.
[52] CAMPUS® 5.0 data base. BASF-2004-05-24 -Ultramid® B3S.
[53] V.K.R. Kodur, M.A. Sultan, Effect of temperature on thermal properties of high-strength concrete, J. Mater. Civ. Eng. 15 (2) (2003) 101–107, https://doi.org/10.1061/(ASCE)0899-1561(2003)15:2(101).
[54] W. Zheng, H. Li, Y. Wang, Compressive behaviour of hybrid fiber-reinforced reactive powder concrete after high temperature, Mater. Des. 41 (2012) 403–409, https://doi.org/10.1016/j.matdes.2012.05.026.
[55] M. Nematzadeh, A. Karimi, S. Fallah-Valukolaee, Compressive performance of steel fiber-reinforced rubberized concrete core detached from heated CFST, Constr. Build. Mater. 239 (2020) 117832, https://doi.org/10.1016/j.conbuildmat.2019.117832.
[56] W. Yonggui, L. Shuaipeng, P. Hughes, F. Yuhui, Mechanical properties and microstructure of basalt fibre and nano-silica reinforced recycled concrete after exposure to elevated temperatures, Constr. Build. Mater. 247 (2020) 118561, https://doi.org/10.1016/j.conbuildmat.2020.118561.
[57] L. Li, R. Zhang, L. Jin, X. Du, J. Wu, W. Duan, Experimental study on dynamic compressive behavior of steel fiber reinforced concrete at elevated temperatures, Constr. Build. Mater. 210 (2019) 673–684, https://doi.org/10.1016/j.conbuildmat.2019.03.138.

[58] O.A. Düzgün, R. Gül, A.C. Aydin, Effect of steel fibers on the mechanical properties of natural lightweight aggregate concrete, Mater. Lett. 59 (27) (2005) 3357–3363, https://doi.org/10.1016/j.matlet.2005.05.071.
[59] S. Yehia, A. Douba, O. Abdullahi, S. Farrag, Mechanical and durability evaluation of fiber-reinforced self-compacting concrete, Constr. Build. Mater. 121 (2016) 120–133, https://doi.org/10.1016/j.conbuildmat.2016.05.127.
[60] D. Choumanidis, E. Badogiannis, P. Nomikos, A. Sofianos, The effect of different fibres on the flexural behaviour of concrete exposed to normal and elevated temperatures, Constr. Build. Mater. 129 (2016) 266–277, https://doi.org/10.1016/j.conbuildmat.2016.10.089.
[61] C. Frazão, J. Barros, A. Camões, A.C. Alves, L. Rocha, Corrosion effects on pullout behavior of hooked steel fibers in self-compacting concrete, Cem. Concr. Res. 79 (2016) 112–122, https://doi.org/10.1016/j.cemconres.2015.09.005.
[62] P. Sukontasukkul, W. Pomchiengpin, S. Songpiriyakij, Post-crack (or post-peak) flexural response and toughness of fiber reinforced concrete after exposure to high temperature, Constr. Build. Mater. 24 (10) (2010) 1967–1974, https://doi.org/10.1016/j.conbuildmat.2010.04.003.
[63] H.R. Pakravan, T. Ozbakkaloglu, Synthetic fibers for cementitious composites: A critical and in-depth review of recent advances, Constr. Build. Mater. 207 (2019) 491–518, https://doi.org/10.1016/j.conbuildmat.2019.02.078.
[64] G.F. Peng, Z.S. Huang, Change in microstructure of hardened cement paste subjected to elevated temperatures, Constr. Build. Mater. 22 (4) (2008) 593–599, https://doi.org/10.1016/j.conbuildmat.2006.11.002.
[65] A. Lau, M. Anson, Effect of high temperatures on high performance steel fibre reinforced concrete, Cem. Concr. Res. 36 (9) (2006) 1698–1707, https://doi.org/10.1016/j.cemconres.2006.03.024.
[66] Y.S. Tai, H.H. Pan, Y.N. Kung, Mechanical properties of steel fiber reinforced reactive powder concrete following exposure to high temperature reaching 800 C, Nucl. Eng. Des. 241 (7) (2011) 2416–2424, https://doi.org/10.1016/j.nucengdes.2011.04.008.
[67] W.P.S. Dias, G.A. Khoury, P.J.E. Sullivan, Mechanical properties of hardened cement paste exposed to temperatures up to 700 C (1292 F), Mater. J. 87 (2) (1990) 160–166.
[68] P. Smarzewski, Study of toughness and macro/micro-crack development of fibre-reinforced ultra-high performance concrete after exposure to elevated temperature, Materials 12 (8) (2019) 1210, https://doi.org/10.3390/ma12081210.